Mechanical Magnetic Field Generator for Communication in the ULF Range

Hossein Rezaei[®], Student Member, IEEE, Victor Khilkevich, Member, IEEE, Shaohui Yong[®], Student Member, IEEE, Daniel Steven Stutts[®],

and David Pommerenke^(D), Fellow, IEEE

Abstract—Electromagnetic (EM) fields at radio frequencies (RF) cannot penetrate deep into media with high conductivity such as sea water, wet soil, etc. However, moving to the ultralow frequency (ULF) range (300 Hz-3 kHz) allows a considerable range of communication due to the decreased medium loss at low frequencies and a possibility to use the penetrating near field. Magnetically coupled coils are commonly used for nearfield magneto-inductive (MI) communication. Alternatively, it is possible to create ULF magnetic fields of sufficient amplitude by rotating permanent magnets. In this work, a ULF magnetic field generator has been created using a rotating permanent magnet. It has been shown that the proposed field generator outperforms a conventional coil source (23 dB of field strength for the same volume and dissipated power that is 0.35 W), which can be a considerable advantage for low size, weight, and power applications. A method to produce amplitude shift keying (ASK) modulation signals using a modulation coil was proposed and analyzed. It was demonstrated that the inductance of the modulation coil is not critical for achieving acceptable modulation ratios, which opens a possibility for a compact ASK generator design. A simple circuit model and analytical formula for modulation efficiency of the generator were proposed and validated by measurement.

Index Terms—Magneto inductive (MI) communication, near field, rotating permanent magnet.

I. Introduction

AGNETO-INDUCTIVE (MI) communication is a technique commonly used for underwater or underground communication or wireless power transmission, in biomedical applications [1]–[8]. In MI communication, the transmission and reception are accomplished using two coils which are normally tuned to resonance to ensure maximum efficiency [9], [10].

Alternatively to the coils, permanent magnets can be used for both receiving [2] and generating [11], [12] the penetrating near field, although the intended applications in [2] and [11] are limited to wireless power transfer and biomedical uses.

In this article, we propose the design of a mechanical magnetic field generator, including the carrier modulation

Manuscript received April 23, 2019; revised September 6, 2019; accepted September 22, 2019. Date of publication November 28, 2019; date of current version March 3, 2020. (Corresponding author: Hossein Rezaei.)

H. Rezaei, V. Khilkevich, S. Yong, and D. Pommerenke are with the Department of Electrical and Computer Engineering, Missouri University of Science and Technology, Rolla, MO 65409-0050 USA (e-mail: hrr7d@mst.edu).

D. S. Stutts is with the Department of Mechanical Engineering, Missouri University of Science and Technology, Rolla, MO 65409-0050 USA.

Color versions of one or more of the figures in this article are available online at http://ieeexplore.ieee.org.

Digital Object Identifier 10.1109/TAP.2019.2955069

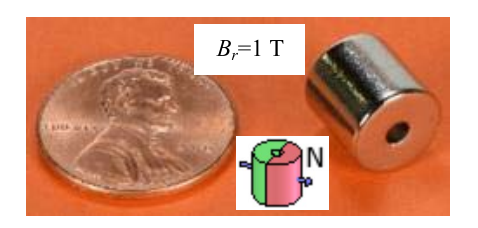


Fig. 1. Diametrically magnetized cylindrical magnet R6036DIA.

method, and compare its efficiency to the conventional coil sources.

II. MI FIELD GENERATOR

A time-changing magnetic field is created each time the orientation of the magnetic moment of the permanent magnet is altered.

The magnetic field of the permanent magnet (at the direction of its magnetic moment) at sufficiently large distances is given by [13]

$$B(r) = \frac{\mu_0 m}{2\pi r^3} \tag{1}$$

where r is the distance from the magnet and m is its magnetic moment. In the quasi-static approximation (which is quite accurate for the near field) the magnetic field vector at the observation point would roughly follow the direction of the magnetic moment vector (at least when the magnetic moment changes direction by 180° , the magnetic field vector would also flip the direction), allowing a time-changing field by changing the orientation of the magnetic moment of the magnet.

The easiest way to create a periodic magnetic field is to rotate a permanent magnet over the axis perpendicular to its magnetic moment. This method was used in the mechanical generator prototype with a diametrically magnetized cylindrical magnet [14] (Fig. 1).

The dimensions of the magnet are the following: outer diameter—3/8 in (9.525 mm), inner diameter—3/32 in (2.38 mm), length—3/8 in (9.525 mm), and the mass is 4.77 g.

As shown in Fig. 2, the magnet is placed on a brass shaft, which is rotated by two high-speed dc motors [15].

The shaft is connected directly to the rotors of the motors, such that the magnet is supported by the bearings of the

0018-926X © 2019 IEEE. Personal use is permitted, but republication/redistribution requires IEEE permission. See https://www.ieee.org/publications/rights/index.html for more information.

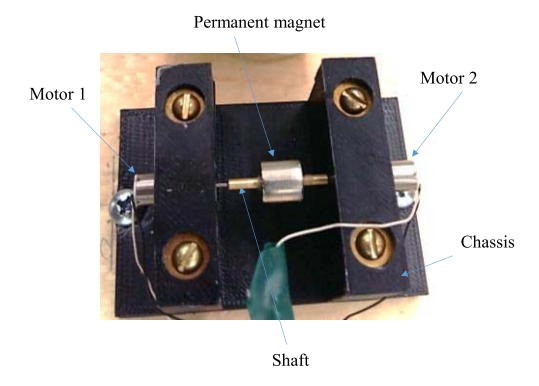


Fig. 2. Prototype of the mechanical magnetic field generator.



Fig. 3. Magnetic field detection coil.

motors. Two motors are used to increase the torque and avoid the need for additional bearings. It should be noted that the permanent magnet should be placed at a considerable distance from the motors (around 1 cm), otherwise the interaction between the rotating magnet and the magnets inside the motors prevents them from running. The entire structure is supported by a plastic chassis. The rotation frequency is determined by the dc voltage applied to the motors and can reach nominally 56 000 r/min, which corresponds to 933 Hz. In the experiments, a frequency close to 700 Hz was reached, which corresponded to 2.5 V dc voltage. Achieving higher rotation speeds requires a well-balanced set-up to avoid excessive vibration

To detect the magnetic field generated by the magnet a simple solenoid coil was used (Fig. 3).

The coil had a diameter of 60 mm and 48 turns of 22 AWG wire.

The probe factor of the coil, defined as the ratio of the magnetic B field at the coil location to the voltage induced at the coil terminals, can be calculated analytically. According to Faraday's law the voltage induced at the terminals of the coil exposed to the uniform magnetic field can we written as follows:

$$v_{coil} = -N \cdot A \frac{dB}{dt} \tag{2}$$

where N is the number of turns in the coil, A is the area of the coil cross section, and B is the magnetic field parallel to the axis of the coil.



Fig. 4. Validation of the receiving coil probe factor using a Helmholtz coil.

For the harmonic magnetic field with complex amplitude B at frequency ω , (2) can be written as follows:

$$v_{coil} = -j\omega BNA \tag{3}$$

and the probe factor is, therefore,

$$A_{coil} = \left| \frac{B}{v_{coil}} \right| = \frac{1}{\omega NA}.$$
 (4)

For the dimensions listed above, the probe factor is $A_{coil} = (7.4/\omega)[\text{T/V}]$. The calculated probe factor was validated using a Helmholtz coil that creates almost a uniform magnetic field close to its axis (Fig. 4). The difference between the actual induced voltage in the receiving coil and predicted using the calculated probe factor was 1.3 dB. Such an error was deemed acceptable.

The magnetic moment of the permanent magnet can be found by integrating the residual magnetization of the magnet B_r over its volume V [2]

$$m = \int_{V} \frac{B_r}{\mu_0} dv. \tag{5}$$

The calculation can be simplified by assuming a uniform residual field inside the volume as follows:

$$m \approx \frac{B_r V}{\mu_0}. (6)$$

Using the average value of the residual field (B_r) for R6036DIA provided by the manufacturer (1 T), the magnetic moment of the magnet can be estimated using (6) as $m = 0.51 \text{ A} \cdot \text{m}^2$.

According to (1), the amplitude of the magnetic field at 1 m from the magnet can be estimated as -140 dBT, which agrees well with the measured value of -141 dBT obtained by measuring the voltage induced in the receiving coil and applying the probe factor to it. The achieved rotation speed of 700 Hz corresponded to 0.35 W of power consumed by the motors. This value will be used as a reference for the efficiency comparison in Section III. Field strength at greater distances can be calculated using (1). The useful communication range can be estimated based on the known sensitivity of the receiver.

III. COMPARISON OF EFFICIENCIES OF COIL AND ROTATING MAGNET MI SOURCES

Of course, similar field intensities can be achieved by a conventional coil structure driven by the sinusoidal current. Furthermore, new coil designs—e.g., metamaterial, ferrite core coils, or MIMO—were proposed recently to enhance the magnetic field or improve channel capacity. The magnetic field of a multiturn coil with a ferrite core can be increased by about 10 dB over its air core counterpart [16]. However, high permeability materials are susceptible to saturation in the presence of strong magnetic fields [17] which does not allow use of these solutions at magnetic field strengths comparable to that of permanent neodymium magnets (around 1 T).

Using metamaterials increases the effectiveness of the coil significantly [18], [19]. Unidirectional [19], bidirectional [20], or tridirectional [21] metamaterial coils can generate up to about a 20 dB stronger field compared to a conventional coil of the same size at a resonance frequency. Nevertheless, intrinsic resonance of metamaterial coils would result in a narrow bandwidth of the communication system and low data exchange rates because of already low carrier frequencies of MI communication (typically hundreds of Hz).

To address this problem MIMO coil antenna arrays are proposed to increase MI communication bandwidth [22]. Each element in the array is resonant at its own frequency, but the antenna array as a whole system has a resonant frequency which might be different from its elements. Although MIMO antenna arrays improve channel capacity in MI communications, the need for multiple coils increases the volume, cost, and complicates the design process of the system.

As will be demonstrated further, the proposed mechanical generator can generate up to about 24 dB stronger magnetic field compared to a conventional coil of the same size, which is comparable with recently reported field enhancement with metamaterial coil (for equal efficiencies) [18], [19]. This might be an important factor for low size, weight, and power applications. In contrast to the metamaterial coils which are designed to work at a resonance frequency with limited bandwidth, the proposed mechanical generator allows tuning the carrier frequency easily just by changing the rotation speed of the dc motors and modulate at fast rates.

The efficiency of the near field generator is difficult to define rigorously because if the radiation loss is neglected (which is the case in this study), such a generator does not dissipate any energy through the magnetic field. Nevertheless, the energy is dissipated in the generator itself (in the motor or in the coil due to the ohmic loss in the wire). Since the role of the generator is to produce the magnetic field of a certain intensity, it makes sense to define the efficiency as the generated field intensity per amount of power lost in the generator. Following this definition, the generators can be compared by, for example, amount of lost power needed to generate fields of equal intensity, or alternatively by the field intensity corresponding to the same power of loss. The latter definition is used further in this study.

Another important parameter is the volume occupied by the generator. It is easy to create a coil that would produce



Fig. 5. Photograph of a typical coil illustrating the parameter definition of the coil model.

a stronger field than the permanent magnets (for equal lost power), but at the expense of occupying a considerably larger volume

This can be demonstrated by considering the following coil model. Suppose a copper wire of diameter D_w is wound around the cylindrical air core of radius R_c in N_t turns and N_l layers (Fig. 5).

The magnetic field generated by each turn at a distance r along the axis of the coil core can be calculated as follows [231:

$$B_t = \frac{\mu_0 I R_t^2}{2(\sqrt{r^2 + R_t^2})^3} \tag{7}$$

where I is the current in the turn and R_t is the turn radius.

Because of the layered structure of the coil model all turns have different radii, and the distance to the observation point is also different due to the length of the coil. In order to simplify the field calculation, the following approximations are used: 1) the distance to the observation point is equal for all turns (which corresponds to the case when the distance to the observation point is much larger than the length of the coil) and 2) the mean turn radius R_m is used for all turns, which is calculated as follows:

$$R_m = \frac{R_{min} - R_{max}}{2} + R_{min} \tag{8}$$

where $R_{min} = R_c - (2t + D_w)/2$ and $R_{max} = R_{min} + N_l(D_w + 2t)$ are the minimum and maximum radii of turns, respectively, and t is the thickness of the insulator which is considered to be 10% of the wire diameter in (8).

The field generated by the coil is, therefore, calculated as follows:

$$B_{coil} \approx \frac{\mu_0 I R_m^2}{2(\sqrt{r^2 + R_m^2})^3} N_t. \tag{9}$$

It is obvious that by increasing the current in the coil, it is possible to achieve any desired field strength. Therefore, to make the comparison to the mechanical source meaningful, the dissipated power in the coil is required to be equal to the power consumed by the rotating magnet source achieved in the experiment described above (0.35 W). This condition ensures equal efficiencies of both sources in terms of dissipated power

per unit of the generated magnetic field (in the case of equal field strength generated).

The current in the coil is therefore calculated as follows:

$$I = \sqrt{P_{magnet}/R_{coil}} \tag{10}$$

where $P_{magnet} = 0.35$ W and R_{coil} is the resistance of the coil wire

$$R_{coil} = \frac{\rho L_w}{A_w} \tag{11}$$

where ρ is the copper resistivity $(1.73 \cdot 10^{-8} \ \Omega \cdot m)$, L_w is the wire length, and $A_w = \pi (D_w/2)^2$ is the cross-section area of the wire. The length of the wire is estimated as follows:

$$L_w = 2\pi R_m \lceil N_t / N_l \rceil \tag{12}$$

where N_t is the number of turns and $\lceil \cdot \rceil$ is the operator of rounding up to the nearest integer which is needed to avoid a physically impossible number of turns (N_t) to number of layers (N_t) ratios below 1.

The volume occupied by the coil is calculated as follows:

$$V_{coil} = A_{coil} L_{coil} (13)$$

where $A_{coil} = \pi [R_{min} + N_l(D_w + 2t)]^2$ is the cross-section area of the coil, $L_{coil} = (D_w + 2t)\lceil N_t/N_l \rceil$ is the length of the coil.

The coil model has therefore four parameters: number of turns N_t , number of layers N_l , wire diameter D_w , and core radius R_c .

The optimal coil design is defined as creating the largest possible magnetic field strength (at a given distance) for a specified volume. Since both field strength (9) and volume (13) are nonlinearly related to the parameters of the coil, analytical optimization is problematic, and a random one is performed instead. To perform the random optimization, all parameters of the coil model are represented as random variables as follows:

$$P_i = 10^{X_i} \tag{14}$$

where the order of magnitude of the parameter $X_i = \text{unif}(X_i^{min}, X_i^{max})$ is the uniformly distributed random number on the interval (X_i^{min}, X_i^{max}) , i.e., all parameters are exponentially distributed (this results in more uniform distribution of designs when plotted in the logarithmic scale). For each combination of parameters, the field strength at a distance of 1 m and the coil volume are calculated.

Eventually 50 000 combinations of the input parameters are analyzed with the limits specified in Table I.

The resulting designs are plotted in Fig. 6 as blue dots on the field intensity/volume chart along with the orange dot representing the rotating magnet field source.

As shown in Fig. 6, the coil of comparable volume would produce the magnetic field which is approximately 24 dB lower than the field generated by the magnet (-164 dBT) versus -140 dBT).

Therefore, the smallest conventional coil capable of producing the field of the same strength (for 0.35 W dissipated power in Fig. 6) would occupy 30 times more space than a rotating magnet $(2 \cdot 10^{-5} \text{ m}^3 \text{ versus } 6.4 \cdot 10^{-7} \text{ m}^3)$.

TABLE I LIMITS OF THE COIL PARAMETERS

Parameter	Minimum order X ^{min}	Maximum order X^{max}	Minimum value P ^{min}	Maximum value <i>P</i> ^{max}
Number of turns	0	2	1	100
Number of layers	0	2	1	100
Wire diameter	-5	-3	0.01 mm	1 mm
Core radius	-2	-1	1 cm	10 cm

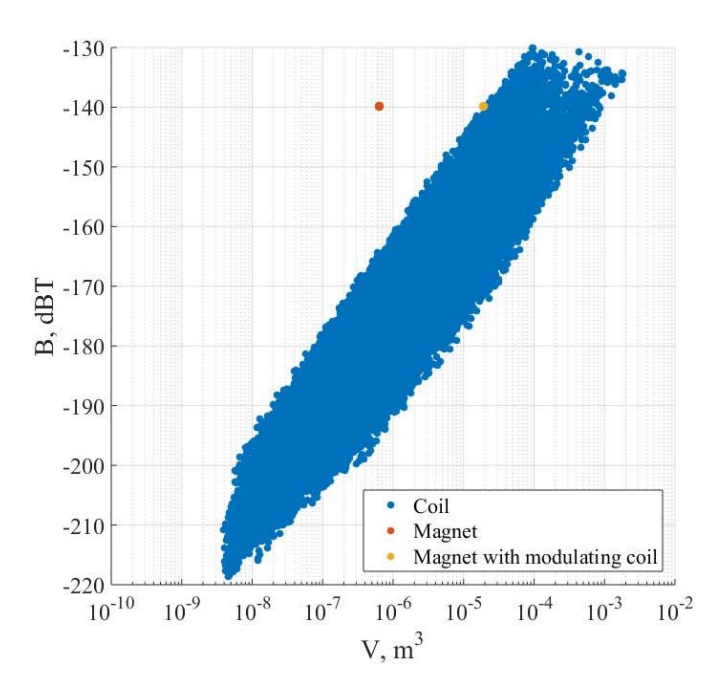


Fig. 6. Comparison of magnet and coil sources in terms of field strength at 1 m and occupied volume.

To organize a bidirectional communication, the system needs to be equipped with a receiver. Potentially the magnet of the mechanical generator can be used as a mechanical detector of magnetic field [12]; however, the feasibility of this approach requires additional investigation. Alternatively, the modulation coil, which is introduced in Section IV, can be used as the receiving antenna. Of course, introduction of the additional coil increases the overall volume occupied by the system.

IV. ASK MODULATION METHOD FOR THE ROTATING MAGNET GENERATOR

The source of continuous sinusoidal signal is virtually useless for communication and requires a modulation method. The easiest way to achieve modulation in the rotating magnet generator is to change the rotation frequency implementing the phase or frequency modulation of the generated signal. However, due to large inertia of the magnet and low torque and power of the high-speed motors, only very small modulation bandwidths can be achieved using this method.

Alternatively, an amplitude modulation (or more precisely, amplitude shift keying—ASK) can be achieved by placing the rotating magnet inside a modulation coil loaded by a variable

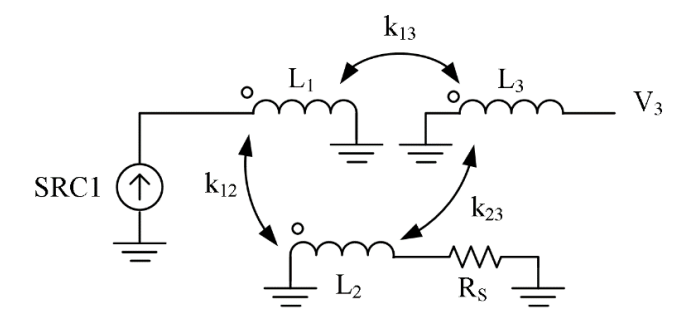


Fig. 7. Model of the AM for the rotating magnet source.

resistor (a switch) such that the magnetic field vector rotates in the longitudinal plane of the coil. The principle of operation of this method is demonstrated by the following analysis.

The magnet placed inside the modulation coil will generate the inductive electromotive force (EMF) in it. The magnet itself is not affected by the coil (assuming that the back EMF effect is neglected). In this case, the magnet can be represented by a coil driven by an ac current source, which is coupled to the modulation coil. Both the magnet and the modulation coil are coupled to the receiving coil. The entire model is shown in Fig. 7.

The inductor L1 driven by the ac current source SRC1 represents the rotating magnet. The inductor L2 (modulation coil) is relatively strongly coupled to the inductor L1 (magnet) and is loaded by the resistor Rs (switch). Both coils L1 and L2 are weakly coupled to the receiving coil L3. The coupling in the circuit is described by the coupling coefficients $k_{12} = M_{12}/\sqrt{L_1L_2}$, $k_{13} = M_{13}/\sqrt{L_1L_3}$, and $k_{23} = M_{23}/\sqrt{L_2L_3}$. Since the coils L1 and L2 are in the vicinity of one another, and the coil L3 is placed at a large distance from both L1 and L2, the following conditions are true: $k_{12} \gg k_{13}$ and $k_{12} \gg k_{23}$.

The current I_1 in the inductor L1 is set by the current source which induces the EMF in the inductor L2; at the same time, the contribution of the current in the inductor L3 to the current in L2 is negligible because of the weak coupling; therefore, the EMF induced in the L2 is

$$V_2 = -j\omega M_{12} I_1 \tag{15}$$

and the current in L2 is

$$I_2 = -\frac{j\omega M_{12}I_1}{R_s + j\omega L_2}. (16)$$

Both currents I_1 and I_2 induce the EMF in the inductor L3

$$V_3 = -i\omega M_{13}I_1 - i\omega M_{23}I_2. \tag{17}$$

By substituting (16) into (17), the EMF V_3 can be expressed as follows:

$$V_3 = I_1 \frac{\omega^2 (M_{13}L_2 - M_{12}M_{23}) - j\omega M_{13}R_s}{R_s + i\omega L_2}.$$
 (18)

Equation (18) describes the steady state amplitude of the voltage induced in the receiving coil, which depends on the resistance of the switch R_s .

Assuming the resistance of the switch is infinite in the open circuit condition $R_{s,oc} = \infty$ and is equal to some constant

value in the short-circuit condition $R_{s,sc} = R_0$ (representing the residual resistance of the switch and the resistance of the modulation coil), two possible amplitudes of the induced voltage can be found as follows:

$$V_{3,sc} = I_1 \frac{\omega^2 (M_{13}L_2 - M_{12}M_{23}) - j\omega M_{13}R_0}{R_0 + j\omega L_2}$$

$$V_{3,oc} = j\omega M_{13}I_1.$$
(19)

Two different amplitudes in (19) allow implementing the ASK modulation with the ratio of values (modulation ratio)

$$K = \frac{V_{3,sc}}{V_{3,oc}} = \frac{(M_{13}L_2 - M_{12}M_{32}) - jM_{13}R_0/\omega}{jM_{13}R_0/\omega - L_2M_{13}}.$$
 (20)

Expressing the mutual inductances through the coupling coefficients shows the modulation ratio is

$$K = \frac{k_{13} \left(1 + \frac{R_0}{j\omega L_2} \right) - k_{12}k_{23}}{-k_{13} \left(1 + \frac{R_0}{j\omega L_2} \right)}.$$
 (21)

Introducing the effective coupling coefficient from the magnet to the receiving coil

$$k'_{13} = k_{13} \left(1 + \frac{R_0}{j\omega L_2} \right) \tag{22}$$

the modulation ratio can be expressed as follows:

$$K = k_{12} \frac{k_{32}}{k'_{13}} - 1. (23)$$

In the case when the resistance of the switch/coil is negligible relative to the reactive impedance of the modulation coil (i.e., when $R_0 \ll |j\omega L_2|$), the modulation ratio becomes

$$K = k_{12} \frac{k_{32}}{k_{13}} - 1. (24)$$

In this situation, the modulation ratio is determined solely by the coupling coefficients between the magnet (L1) and modulation coil (L2), between both of them to the receiving coil (L3), and does not depend on coil inductances. In practice, the short circuit resistance is not always negligible, which increases the absolute value of the modulation ratio (23) (i.e., makes the modulation less efficient) relative to (24).

The ratio between the amplitudes (23) can be related to the modulation index, which is the ratio between the modulation amplitude (or half difference between the modulation levels $M = (V_{3,oc} - V_{3,oc}K)/2 = V_{3,oc}(k_{12}k_{23})/2$) and the carrier amplitude (or the average between two modulation levels $A = (V_{3,oc} + V_{3,oc}K)/2 = V_{3,oc}(2k'_{13} - k_{12}k_{23})/2$) as follows:

$$m_A = \frac{M}{A} = \frac{1 - K}{1 + K} = \frac{k_{12}k_{23}}{2k'_{13} - k_{12}k_{23}}.$$
 (25)

The analysis presented above is simplified, as it does not take into account transitions between the high/low impedances in the modulation coil and assumes steady state signals for both states of the modulation coil (short and open). However, as numerical simulation of circuit in Fig. 7 shows, the accuracy of estimation (25) is good. For example, the first harmonic of the sideband of the voltage in the receiving coil V_3 obtained numerically for $R_0 = 0$, $k_{12} = 0.8$, $k_{13} = k_{23} = 1 \cdot 10^{-4}$ with

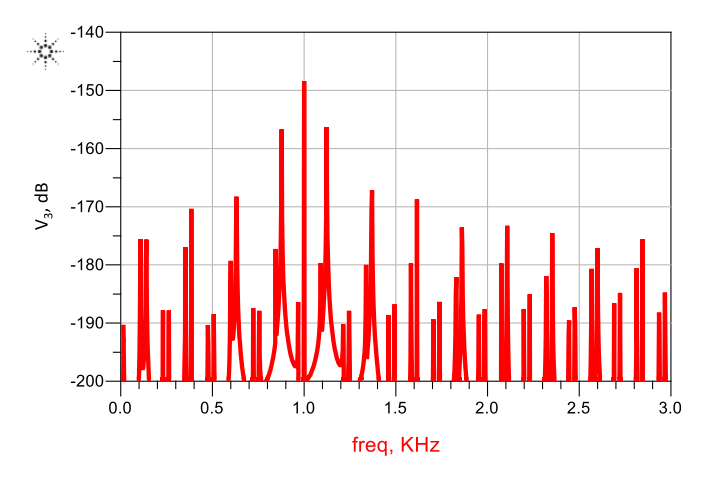
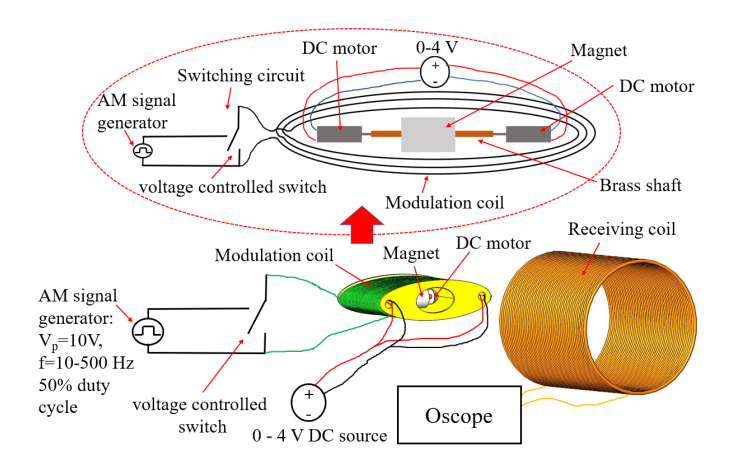


Fig. 8. Spectrum of the AM voltage in the receiving coil for $R_0=0$, $k_{21}=0.8$, $f_c=1$ kHz, $f_{AM}=123$ Hz, and 50% duty cycle. Obtained using the transient analysis.



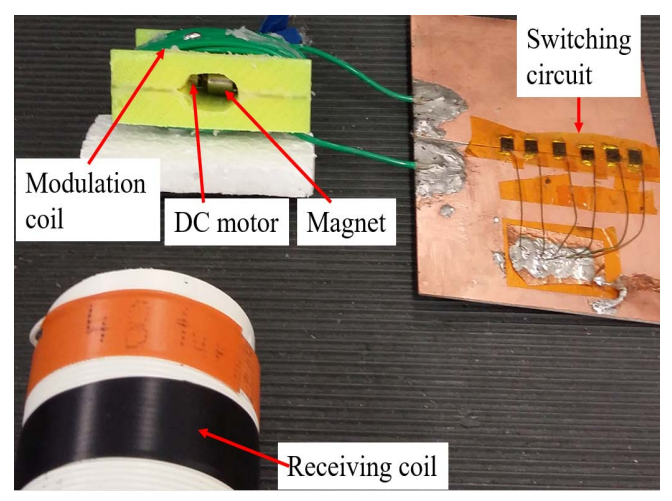


Fig. 9. ASK modulation prototype.

 $f_c = 1$ kHz and $f_{AM} = 123$ Hz, and 50% duty cycle has a value of -7.5 dBc as Fig. 8 demonstrates.

A similar value can be determined using the approximated analysis presented above. In a one-tone AM modulation, the carrier to sideband ratio is $m_{AM}/2$. In the circuit at Fig. 7, the modulation is performed using a rectangular signal, which

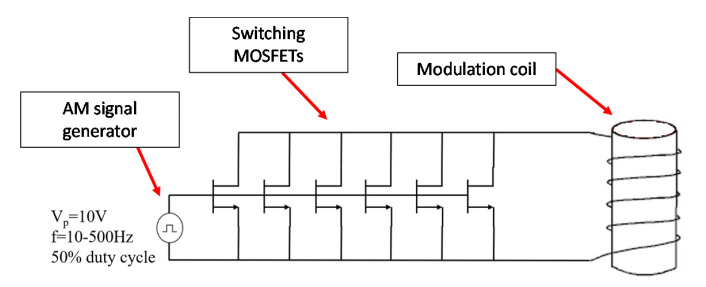


Fig. 10. Circuit for the ASK modulation.

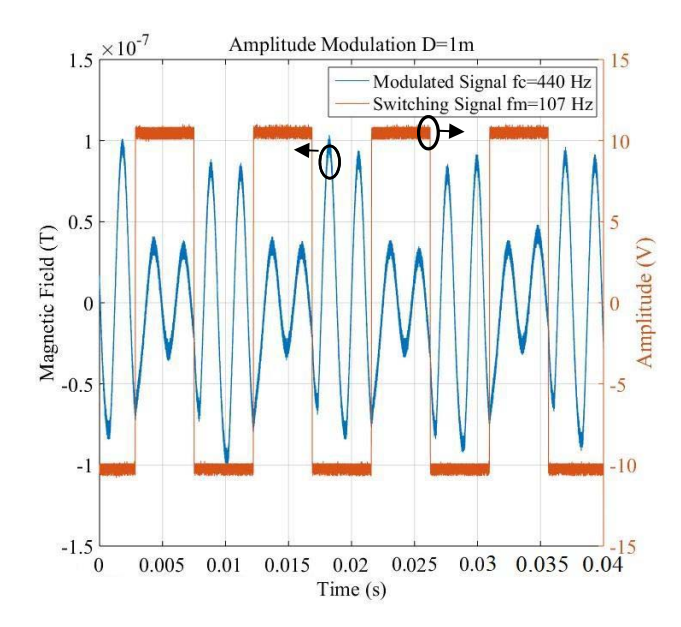


Fig. 11. Measured time domain waveform of the AM signal.

has an increased amplitude of the first harmonic compared to the sinusoidal signal of the same amplitude. The value of the first harmonic of the rectangular waveform of amplitude M is $M_1 = (4M/\pi)\sin\pi(t_p/T)$, where t_p is the pulsewidth, and T is the period of the signal. For the 50% duty cycle signal with unit amplitude, the first harmonic amplitude is: $M_1 = (4/\pi)$. Therefore, the relative amplitude of the first harmonic of the sideband estimated using (25) for $k_{21} = 0.8$ is $S_1 = (m_A/2)M_1 = (k_{12}k_{23}/2k_{13} - k_{12}k_{23})(2/\pi) = 0.42$, corresponding to -7.44 dBc, which is very close to the value obtained by a circuit simulator.

To test the ASK modulation method described above, the rotating magnet was placed inside the coil as illustrated in Fig. 9. The coil in Fig. 9 was shorted by the parallel channels of six low-channel resistance MOSFETS (TPHR6503PL, on-channel resistance 0.4 m Ω), driven by the signal generator at 10–500 Hz as shown in Fig. 10.

A typical signal induced in the receiving coil in the set-up in Fig. 9 is shown in Fig. 11, demonstrating ASK modulation. As shown in Fig. 11, frequency of the carrier and the modulation signals are about 440 and 107 Hz, respectively, with a modulation ratio of about 0.32.

Even though no optimization of the ASK prototype was performed, the size of prototype $(1.88 \cdot 10^{-5} \text{ m}^3)$ is close to

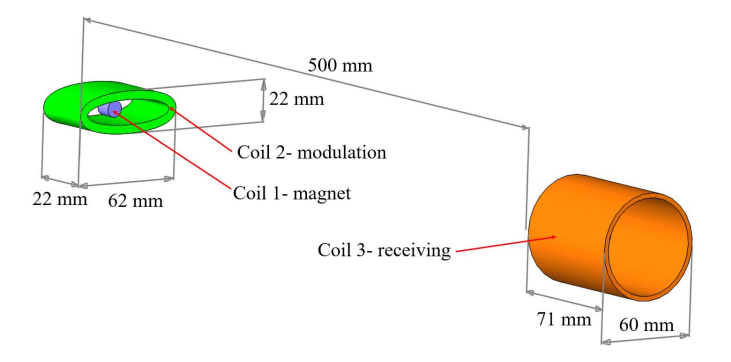


Fig. 12. EM model for the coupling coefficient calculation.

the smallest coil $(1.8 \cdot 10^{-5} \text{ m}^3)$ capable of producing the field of the same strength (see Fig. 6). Further minimization of the modulation system might create the mechanical source out-performing the conventional MI coil. Knowing that the modulation ratio in ideal circumstances does not depend on the inductance of the modulation coil, it might be possible to create the effective ASK system even with smaller modulation coil. An obvious solution would be to wind the modulation coil as close to the magnet as possible. However, as experiments show, when the modulation coil becomes too strongly coupled to the magnet, the inductive force applied to the magnet when the modulation coil is switched becomes too strong, which leads to undesirable effects such as carrier frequency decrease, increased power consumption, and parasitic frequency modulation.

V. ESTIMATION OF THE COUPLING BETWEEN THE MAGNET AND THE MODULATION COIL

In order to design the magnetic generator with ASK the coupling coefficients k_{12} , k_{13} , k_{23} need to be estimated. This can be achieved using electromagnetic (EM) simulation. A magnetostatic solver in CST [24] can be used to determine the coupling coefficients in a model shown in Fig. 12.

The model corresponds to the prototype in Fig. 9, with three coaxial coils. Coils 2 and 3 reproduce the dimensions of the modulation and receiving coil, and coil 1—roughly the dimensions of the magnet (the magnet shape cannot be modeled exactly because its magnetic moment rotates perpendicular to the magnet symmetry axis).

The simulation in Fig. 12 resulted in the following values of the coupling coefficients: $k_{12} = 0.14$, $k_{23} = 0.0376$, and $k_{13} = 48 \cdot 10^{-4}$. The inductance of the modulation coil is 34.3 μ H and its resistance is 26 m Ω . Using the values above, the absolute value of the modulation ratio was calculated according to (23). Also, the modulation ratio was measured by recording waveforms similar to one in Fig. 11 at different carrier frequencies. Both measured and calculated ratios are presented in Fig. 13.

As Fig. 13 demonstrates, the EM simulation with (23) estimates the modulation ratio with acceptable accuracy.

VI. CONCLUSION

Analysis of the rotating permanent magnet in terms of its efficiency was conducted. It was demonstrated that the rotating

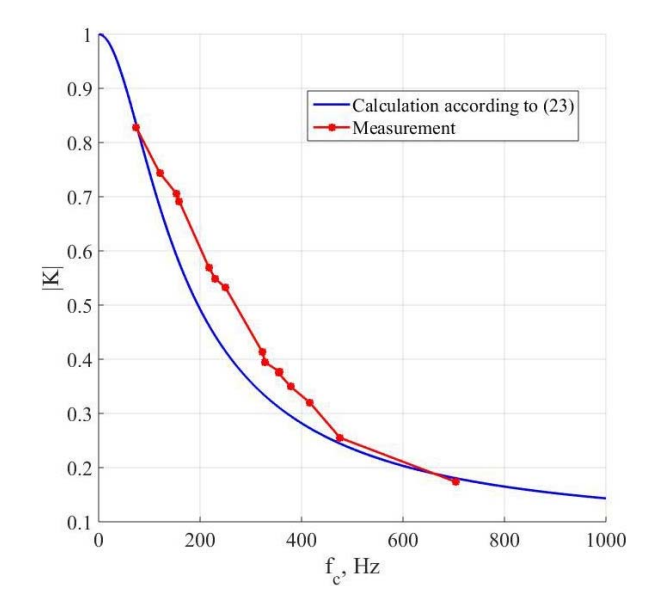


Fig. 13. Measured and calculated modulation ratio.

magnet source outperforms a conventional coil source by a large margin (23 dB of field strength for the same volume and dissipated power), which might be a considerable advantage for low size, weight, and power applications.

A method to produce ASK signals using a modulation coil was proposed and analyzed. It was demonstrated that the inductance of the modulation coil is not critical for achieving acceptable modulation ratios, which opens a possibility for a compact ASK generator design. A simple circuit model and analytical formula for modulation efficiency of the generator were proposed and validated by measurement. Besides modulation, the modulation coil can be used as a receiving antenna in a bidirectional communication system.

Modulation coil increases the overall volume of the system, reducing its efficiency to the levels comparable to that of the conventional coil generator. Further optimization of the system is needed to surpass the coil generator efficiency.

REFERENCES

- M. C. Domingo, "Magnetic induction for underwater wireless communication networks," *IEEE Trans. Antennas Propag.*, vol. 60, no. 6, pp. 2929–2939, Jun. 2012.
- [2] V. R. Challa, J. Oscar, M. Miranda, and D. P. Arnold, "Wireless power transmission to an electromechanical receiver using low-frequency magnetic fields," *Smart Mater. Struct.*, vol. 21, no. 11, Oct. 2012, Art. no. 115017.
- [3] A. Kurs, A. Karalis, R. Moffatt, J. D. Joannopoulos, P. Fisher, and M. Soljačić, "Wireless power transfer via strongly coupled magnetic resonances," *Science*, vol. 317, no. 5834, pp. 83–86, 2007.
- [4] F. C. Flack, E. D. James, and D. M. Schlapp, "Mutual inductance of air-cored coils: Effect on design of radio-frequency coupled implants," *Med. Biol. Eng.*, vol. 9, no. 2, pp. 79–85, Mar. 1971.
- [5] R. Bansal, "Near-field magnetic communication," *IEEE Antennas Propag. Mag.*, vol. 46, no. 2, pp. 114–115, Apr. 2004.
- [6] C. Bunszel, "Magnetic induction: A low-power wireless alternative," RF Design, vol. 24, no. 11, pp. 78–80, 2001.
- [7] M. P. Theodoridis and S. V. Mollov, "Distant energy transfer for artificial human implants," *IEEE Trans. Biomed. Eng.*, vol. 52, no. 11, pp. 1931–1938, Nov. 2005.

- [8] G. Wang, W. Liu, M. Sivaprakasam, and G. A. Kendir, "Design and analysis of an adaptive transcutaneous power telemetry for biomedical implants," *IEEE Trans. Circuits Syst. I, Reg. Papers*, vol. 52, no. 10, pp. 2109–2117, Oct. 2005.
- [9] Z. Sun and I. F. Akyildiz, "Underground wireless communication using magnetic induction," in *Proc. IEEE Int. Conf. Commun.*, Jun. 2009, pp. 4234–4238.
- [10] N. de N. Donaldson and T. A. Perkins, "Analysis of resonant coupled coils in the design of radio frequency transcutaneous links," *Med. Biol. Eng. Comput.*, vol. 21, no. 5, pp. 612–627, 1983.
- [11] H. Jiang *et al.*, "A low-frequency versatile wireless power transfer technology for biomedical implants," *IEEE Trans. Biomed. Circuits Syst.*, vol. 7, no. 4, pp. 526–535, Aug. 2013.
- [12] O. C. Fawole and M. Tabib-Azar, "An electromechanically modulated permanent magnet antenna for wireless communication in harsh electromagnetic environments," *IEEE Trans. Antennas Propag.*, vol. 65, no. 12, pp. 6927–6936, Dec. 2017.
- [13] A. J. Petruska and J. J. Abbott, "Optimal permanent-magnet geometries for dipole field approximation," *IEEE Trans. Magn.*, vol. 49, no. 2, pp. 811–819, Feb. 2013.
- [14] K&J Magnetics. [Online]. Available: https://www.kjmagnetics.com/ proddetail.asp?prod=R6036DIA
- [15] NdFeB HM Motor Large Torque 615 Hollow Cup Motor 3.4-3.7V 52000-56000 RPM Hot. [Online]. Available: https://www.ebay.com/i/ 322427122000?chn=ps
- [16] R. DeVore and P. Bohley, "The electrically small magnetically loaded multiturn loop antenna," *IEEE Trans. Antennas Propag.*, vol. AP-25, no. 4, pp. 496–505, Jul. 1977.
- [17] B. E. Huey and A. L. Anderson, "Active field cancellation to prevent saturation in ferromagnetic-core loop antennas," *IEEE Trans. Electromagn. Compat.*, vol. 60, no. 6, pp. 1686–1694, Dec. 2018.
- [18] Y. Cho et al., "Thin hybrid metamaterial slab with negative and zero permeability for high efficiency and low electromagnetic field in wireless power transfer systems," *IEEE Trans. Electromagn. Compat.*, vol. 60, no. 4, pp. 1001–1009, Aug. 2018.
- [19] H. Guo, Z. Sun, J. Sun, and N. M. Litchinitser, "M²I: Channel modeling for metamaterial-enhanced magnetic induction communications," *IEEE Trans. Antennas Propag.*, vol. 63, no. 11, pp. 5072–5087, Nov. 2015.
- [20] V. P. Pathak, V. Kumar, and R. K. Barik, "Magnetic induction communication based transceiver coil and waveguide structure modeling for non-conventional WSNs," in *Proc. 9th Int. Conf. Comput., Commun. Netw. Technol. (ICCCNT)*, Jul. 2018, vol. 60, no. 6, pp. 1–7.
- [21] H. Guo and Z. Sun, "Full-duplex metamaterial-enabled magnetic induction networks in extreme environments," in *Proc. IEEE Conf. Comput. Commun.*, Apr. 2018, pp. 558–566.
- [22] H.-J. Kim, J. Park, K.-S. Oh, J. P. Choi, J. E. Jang, and J. W. Choi, "Near-field magnetic induction MIMO communication using heterogeneous multipole loop antenna array for higher data rate transmission," *IEEE Trans. Antennas Propag.*, vol. 64, no. 5, pp. 1952–1962, May 2016.
- [23] F. Fiorillo, Measurement and Characterization of Magnetic Materials, 1st ed. Amsterdam, The Netherlands: Elsevier, 2004, pp. 106–108.
- [24] Magneto-Static Solver in CST. [Online]. Available: https://www.cst.com/ products/cstems/solvers/solvermagnetostatics



Victor Khilkevich (M'08) received the Ph.D. degree in electrical engineering from the Moscow Power Engineering Institute, Technical University, Moscow, Russia, in 2001.

He is currently an Associate Research Professor with the Missouri University of Science and Technology, Rolla, MO, USA. His research interests include microwave imaging, automotive electromagnetic compatibility modeling, and high-frequency measurement techniques.



Shaohui Yong (S'17) received the B.S. degree in electrical engineering from Beijing Jiaotong University, Beijing, China, in 2013, and the M.S. degree in electrical engineering from the Missouri University of Science and Technology (formerly University of Missouri—Rolla), Rolla, MO, USA, in 2015, where he is currently pursuing the Ph.D. degree in electrical engineering with the Electromagnetic Compatibility (EMC) Laboratory.

His research interests include signal integrity in high-speed digital systems, electromagnetic interfer-

ence, EMC measurement methods.



Daniel Steven Stutts was born in Canton, GA, USA, in 1959. He received the B.S. and M.S. degrees in mechanical engineering from Louisiana State University, Baton Rouge, LA, USA, in 1983 and 1987, respectively, and the Ph.D. degree in mechanical engineering from Purdue University, West Lafayette, IN, USA, in 1990.

In 1991, he joined the Faculty of Mechanical and Aerospace Engineering, Missouri University of Science and Technology, Rolla, MO, USA, and was promoted to an Associate Professor in 1997. He has

been working in the areas of vibrations, piezoelectric actuator and transducer design and modeling, embedded systems, and coupled field applications since 1991. He is currently a national-class master's bicycle racer.



Hossein Rezaei (S'17) received the B.E. degree in electrical engineering from Islamic Azad University Najafabad Branch (IAUN), Najafabad, Iran, in 2004, and the M.S. degree in electrical engineering from the Shiraz University of Technology (SUTech), Shiraz, Iran, in 2011. He is currently pursuing the Ph.D. degree in electrical engineering with the Electromagnetic Compatibility (EMC) Laboratory, Missouri University of Science and Technology, Rolla, MO, USA.

His research interests include EMC, signal integrity, electromagnetic susceptibility, RF desense, or numerical simulations.



David Pommerenke (F'15) received the Diploma and Ph.D. degrees from the Technical University of Berlin, Berlin, Germany, in 1989 and 1995, respectively.

He worked at Hewlett Packard, Roseville, CA, USA, for five years. He joined the Electromagnetic Compatibility Laboratory, Missouri University of Science and Technology, Rolla, MO, USA, in 2001. He joined ESDEMC, Rolla, in 2019, as a CTO. He has authored more than 150 journal articles and holds 13 patents. His research interests are system-

level electrostatic discharge (ESD), electronics, numerical simulations, EMC measurement methods, and instrumentations.

Dr. Pommerenke is an Associate Editor of TEMC.